

## Estimation of the Passivation of Steel Embedded in Alternative Concrete using a Galvanostatic Pulse Technique

W. Aperador<sup>1,\*</sup>, A. Delgado<sup>1</sup>, J. Bautista-Ruiz<sup>2</sup>

<sup>1</sup> School of Engineering, Universidad Militar Nueva Granada, Bogotá-Colombia

<sup>2</sup> Universidad Francisco de Paula Santander, San José de Cúcuta, Colombia

\*E-mail: [william.aperador@unimilitar.edu.co](mailto:william.aperador@unimilitar.edu.co)

*Received:* 13 April 2015 / *Accepted:* 17 May 2015 / *Published:* 27 May 2015

---

One of the techniques frequently used to measure corrosion in concrete in both laboratory and field evaluations is the galvanostatic pulse technique. This technique provides an alternative evaluation, which has substantial advantages with respect to the most commonly used techniques due to it is linear polarization resistance and control over the applied current, thus minimizing noise problems in the measurement of small polarization potentials. These advantages impart the galvanostatic pulse technique with robustness and reliability in calculating the resistance polarization and other variables. In this work, galvanostatic pulse measurements were applied to concrete of steel slag and alkali-activated fly ash subjected to accelerated carbonation processes by exposing the specimens in a carbonation chamber with 3% carbon dioxide at 65% relative humidity for different times, with full carbonation of concrete to determine the resistance between the reinforcement and a handheld electrode system at the concrete surface due to the entry of carbon dioxide.

---

**Keywords:** corrosion, steel slag, fly ash, carbonation, concrete surface

### 1. INTRODUCTION

The galvanostatic pulse technique was first used for this purpose in 1994 by Elsener [1], but it was not until 2010 that the technique was tested in the field, providing satisfactory results. To study the system, a Randles equivalent circuit, which consists of an ohmic resistance in series with a parallel circuit combined with a capacitor modelling the double layer capacitance and a resistor simulating the polarization resistance, is used [2].

This technique induces a potential, and the response is induced in three parts: the first is related to the electrolyte concrete, which is known as the ohmic resistance and is found in a small moment of time on the order of microseconds [3]. The second is the capacitor, which corresponds to the charging

of the double layer. This step can provide the information needed to determine the reactions that generate corrosion. The third is the polarization resistance, which indicates the resistance that is opposing the passage of ions at the concrete-steel interface [4]. Only the ohmic resistance values ( $R_{\Omega}$ ) and the polarization resistance ( $R_p$ ) must be known because these parameters are involved in this type of study. Moreover, before starting galvanostatic pulse measurements, the technique measures the resting potential before the pulse is generated [3-5].

Carbonation occurs spontaneously by the action of atmospheric carbon dioxide ( $\text{CO}_2$ ) [6]. The carbonation of concrete is not always linked to the type of cement [7]. The penetration of carbonation in cements with steel slag, fly ash, and even in Portland cement is based on a number of internal and external factors, including the hydration conditions, age, the water content of the concrete and its mechanical strength [8-9].

Carbonation is one of the major causes of the deterioration of reinforced concrete structures in places with high levels of  $\text{CO}_2$ , such as city centres and parking buildings [10]. Given the level of air pollution in capital cities and their high levels of  $\text{CO}_2$ , many concrete structures suffer advanced degrees of carbonation. In studies of the pathology of buildings and bridges in capital cities, some elements show corrosion deterioration of reinforcing steel due to carbonation, and this has advanced in some elements more than expected [11].

Due to the high porosity of cement pastes, there is a high water-cement ratio [12]. Carbonation increases as the water-cement ratio increases. In addition, carbonation is amplified by decreasing the amount of cement and the consequent decrease in alkaline reserves [13-14]. The rate of carbonation depends on the type of cement. Cements blended with pozzolanic materials are the most common cements worldwide, but these cements are produced with less calcium hydroxide and therefore less alkaline reserves [15].

Pozzolanic materials, such as fly ash, silica fume, metakaolin, and slag, react with calcium hydroxide (CH) to produce calcium silicate hydrate (SCH) [16]. SCH has higher mechanical and chemical resistance than CH and is less porous. As a result of the pozzolanic reaction, the concrete has higher strength and lower permeability but a lesser amount of calcium hydroxide [17]. However, the remaining amount of calcium hydroxide is sufficient for maintaining highly alkaline conditions in the concrete, and the pH is virtually unchanged even though the reserve alkalinity is reduced [18].

The purpose of this work is to study the loss of passivation of steel embedded in concrete made from steel slag and alkali-activated fly ash. The galvanostatic pulse technique allowed electrochemical characterization, providing accurate values of the behaviour of the steel.

## 2. EXPERIMENTAL DETAILS.

The steel used is ASTM A706 commercial structural steel. This specification covers corrugated low alloy steel bars cut to lengths of 30 cm and intended for applications that require restrictive mechanical properties. The chemical composition of the materials was determined by X-ray fluorescence (Table 1).

**Table 1.** Chemical composition of ASTM A 706 steel.

Element	% Composition
Fe	97.636
Mn	1.42
C	0.31
Si	0.54
S	0.053
P	0.041

As cementitious materials, two compounds were used: one based on type F fly ash from the Termopaipa power plant, whose chemical composition is presented in Table 2. The ignition loss was 5.26% of the total mass determined by calcination of the sample at 1000 ° C, a value associated principally with remnants of unburned carbon [19]. Additionally, the percentage of reactive silica fly ash was evaluated, following the procedure described in UNE 80-225-93, yielding a value of 45.23% by mass. The calculated density is 2.3 g/cm<sup>3</sup>. The fineness was determined by a direct method using the Blaine test of permeability to obtain a value of 6836 cm<sup>2</sup>/g [3]. The other cementitious material used was steel blast furnace slag (GBFS), with the chemical composition shown in Table 2, with coefficients of basicity ( $\text{CaO} + \text{MgO} / \text{SiO}_2 + \text{Al}_2\text{O}_3$ ) of 1.0 and a quality of 1.73 ( $\text{CaO} + \text{MgO} + \text{Al}_2\text{O}_3 / \text{SiO}_2 + \text{TiO}_2$ ). The alkaline activator of a solution of sodium silicate was used at a concentration of 5%, expressed as the Na<sub>2</sub>O slag weight percent (ASTM C 989-99).

**Table 2.** Chemical composition of the granulated blast furnace slag and fly ash.

Compound	Fly ash (Mass %)	Granulated blast furnace slag (Mass %)
SiO <sub>2</sub>	54.3	33.7
Al <sub>2</sub> O <sub>3</sub>	22.8	12.8
Fe <sub>2</sub> O <sub>3</sub>	5.8	0.48
CaO	6.9	45.4
MgO	0.8	1
Na <sub>2</sub> O	0.9	0.12
K <sub>2</sub> O	1.7	1.5
P <sub>2</sub> O <sub>5</sub>	0.7	
TiO <sub>2</sub>	1.6	0.5
MnO	0.01	-
SO <sub>3</sub>	0.92	-
SiO <sub>2</sub> /Al <sub>2</sub> O <sub>3</sub>	3.5	2.63

The type, composition, and size of the fine and coarse aggregates were identical for both types of concrete. Gravel corresponded to a maximum size of 19 mm, specific gravity of 2.94 g /cm<sup>3</sup>,

compact unit mass of  $1.86 \text{ kg/cm}^3$ , loose unit weight of  $1.70 \text{ kg/cm}^3$ , and absorption of 1.3%. Sand corresponded to a specific surface area of  $2.47 \text{ g/cm}^3$ , compact unit mass of  $1.67 \text{ kg/cm}^3$ , loose unit weight of  $1.58 \text{ kg/cm}^3$ , and absorption of 2.9%. Finally, the fly ash was cured for 24 hours in an oven at  $80 \text{ }^\circ\text{C}$  and was subsequently placed in a curing pool for 28 days. The activated slag was placed in a controlled curing atmosphere with 90% relative humidity and a constant temperature of  $20 \text{ }^\circ\text{C}$ .

Two types of concrete samples were formed: one corresponds to 100% alkali-activated slag steel (GBFS), and the other is 100% alkali-activated fly ash.

With the aim of studying the phenomenon of corrosion of steel embedded in concrete under various conditions, the study conditions corresponded to the environment in which the test pieces were immersed for all analyses. The process for measuring the progress of corrosion due to the inclusion of carbon dioxide was performed in a carbonation chamber with controlled conditions (3%  $\text{CO}_2$ , 65% relative humidity and a temperature of  $20^\circ\text{C}$ ). To compare the results obtained by carbonation, the measured specimens were exposed to an environment with the following conditions: 68% RH,  $28 \text{ }^\circ\text{C}$  and 0.03%  $\text{CO}_2$  [20].

Galvanostatic pulse (GP) was used for the electrochemical characterization using a Gamry potentiostat/galvanostat 3000 with a cell composed of a graphite counter electrode, a  $\text{Cu/CuSO}_4$  reference electrode and an ASTM A 706 structural steel working electrode with an exposed area of  $10 \text{ cm}^2$ . Electrochemical measurements were performed for the concrete of the steel slag and fly ash at 0, 500, 1000, 1500 and 2000 hours of exposure. The bias current was  $100 \text{ } \mu\text{A}$ , and the exposure time was 20 seconds [21].

The raw material was characterized before and after alkaline activation by X-ray diffraction (XRD) using a Goniometer PW3050 / 60 ( $\theta / \theta$ ) operated under a XPERT-PRO system with monochromatic Cu K.alpha radiation ( $1.54 \text{ \AA}$ ), operated at 40 kV and 40 mA at  $25 \text{ }^\circ\text{C}$ . The sweep over the surface was from  $2\theta = 20.01^\circ$  to  $2\theta = 99.99^\circ$  with a step  $2\theta = 0.02^\circ$  and a sweep time of 1 second. The crystalline phases of the surface of the steel were determine using the database of the diffraction equipment and the MAUD program, which uses the Rietveld method of adjusting a theoretical pattern to coincide with the observed results. Such theoretical patterns are obtained based on the structures and crystalline parameters.

### 3. RESULTS

#### 3.1 Material Characterization by XRD

The X-ray diffraction pattern for fly ash is presented in its initial condition, i.e., without activation (Figure 1). In this pattern, an amorphous region and a crystalline structure are observed. Its components are mullite and quartz. To quantify the various mineral phases present in the material, including the vitreous fraction, the Rietveld method was applied and indicated that there is 79.3% vitreous phase, 8.21% mullite and 12.49% quartz. Upon activation of the fly ash concrete, mineralogical characterization was performed (Figure 1, blue line), identifying the crystalline compounds and subsequently quantifying the mineral phases present in the material, including vitreous

or amorphous fractions. The activating solution generates a modification of the amorphous phase in the range from 20° to 70°. These characteristic peaks correspond to the formation of aluminosilicate generated through the alkali activation reaction. The new phase is chabazite - Na with a ratio of silica to aluminium equal to 2 [22]. This phase is generated due to the activator solution and thermal curing. The same phases are obtained in the material without alkali activation; however, peaks appear in more definite forms, decreasing the vitreous phase.

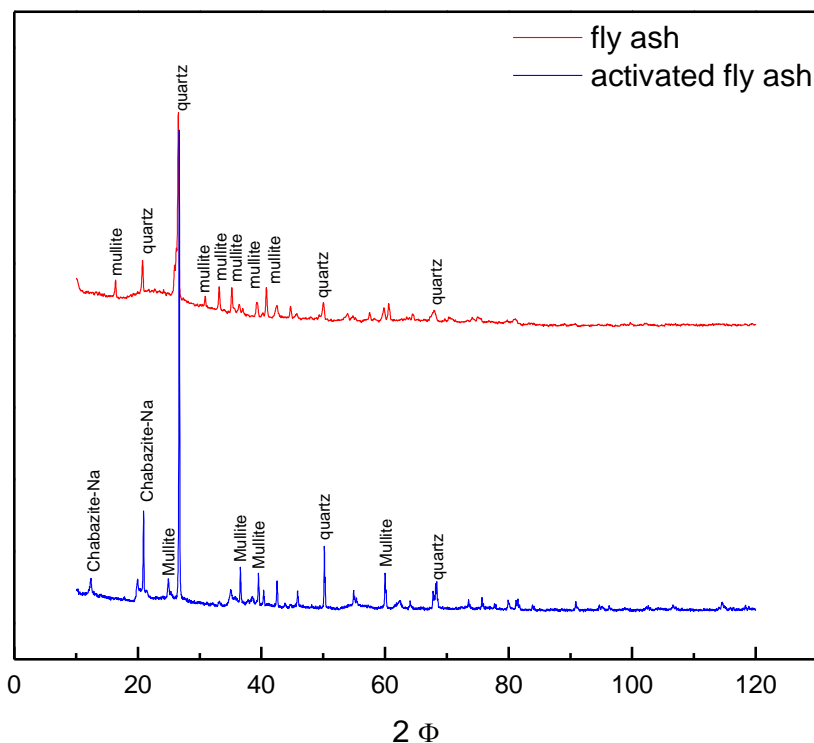


**Figure 1.** X-ray diffractogram corresponding to the fly ash, with and without alkali activation.

The phases of the steel slag included both vitreous and crystalline phases. The grain size is between 48 and 65 μm and includes the following oxides: SiO<sub>2</sub>, Al<sub>2</sub>O<sub>3</sub>, MgO and Fe<sub>2</sub>O<sub>3</sub> (Figure 2). In Table 3, the concentrations of the oxides are shown. The phases are established due to the arrangement of octahedral and tetrahedral MgO molecules. The other phase is silice, a major contaminant of steel, which when combined with lime forms silicates [23].

X-ray diffractograms of the activated steel slag are shown in Figure 3, wherein an amorphous material is obtained that is suitable for the preparation of the concrete. The slag required a vitreous state of more than 90%.

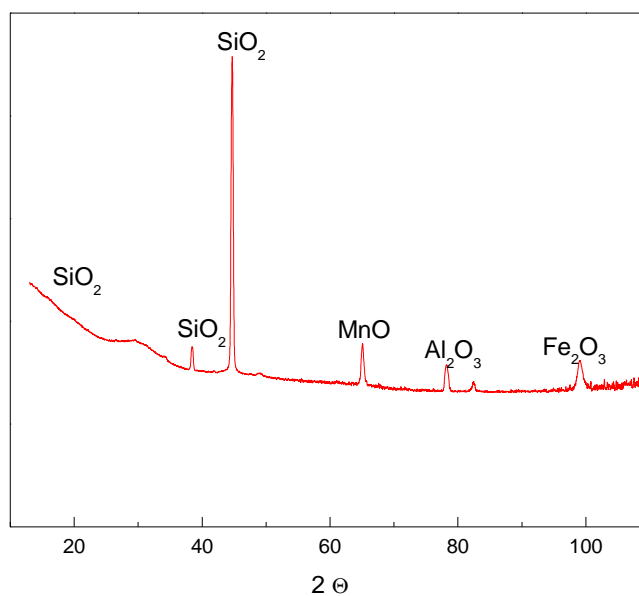


**Figure 2.** X-ray diffractogram corresponding to the steel slag without activating alkali.

**Table 3.** Composition of the steel slag without activation.

Element	% Composition
<b>SiO<sub>2</sub></b>	45.95
<b>Al<sub>2</sub>O<sub>3</sub></b>	12.24
<b>Fe<sub>2</sub>O<sub>3</sub></b>	34.36
<b>MgO</b>	7.45

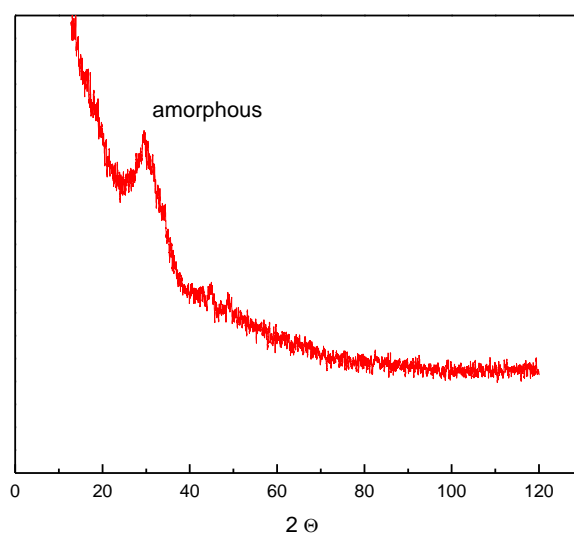


**Figure 3.** X-ray diffraction pattern of the steel slag after the alkali activation.

3.2. Electrochemical assessment

The galvanostatic pulse response is observed for the particular activated fly ash subjected to accelerated carbonation by exposure to 30,000 ppm of carbon dioxide at a temperature of 25 °C. There is a decreasing value of polarization resistance as the carbonation process advances, which is due to the effect of CO<sub>2</sub> in the analysed system. For this reason, the ohmic value corresponding to concrete electrolyte resistance also decreases; therefore, its value is observed in the effect of carbonation in the loss of the electrochemical properties of the analysed system (Figure 4). When studying the concrete with fly ash obtained under 30 ppm carbon dioxide at an average temperature of 25 °C, the material tends to increase its electrochemical components because the shapes of the curves tend to increase their potential, thereby increasing the values of the electrochemical responses. In Table 4, the values of the parameters found after a galvanostatic pulse is applied to the two systems are presented, as described in Figure 4 [24]. The first value discussed refers to the two types of evaluated fly ash concrete exposed to the two means of assessment, which correspond to the ohmic resistance. The provided concrete electrolyte presents a variation because it records a high value at the beginning of the evaluation. At the midpoint of the evaluation, a decline began that continued until the end of the analysis. This fluctuation of the system may be due to the reactions of the cementitious material producing a variation in the resistance value of the electrolyte. For concrete with fly ash exposed to conditions without acceleration, the polarization resistance exhibits an increase. This increase is due to the reactions of the system still being generated, which is beneficial because it increases the analysed parameters. The corrosion potential shows a trend towards more positive potentials, which is appropriate because it shows passivity in the steel.

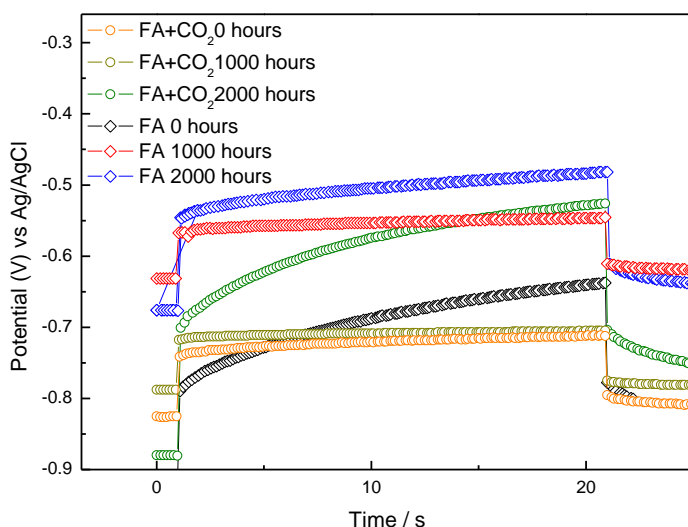


**Figure 4.** Galvanostatic pulse of the fly ash concrete with and without exposure to CO<sub>2</sub>

Comparing the curves of the galvanostatic pulse technique subjected to accelerated carbonation and environmental exposure shows that the concrete subjected to 30,000 ppm carbon dioxide has a potential response at 0 hours. This behaviour indicates that the values of its parameters decrease due to

the effect of accelerated carbonation. Compared with the system exposed to natural environmental conditions, the response in potential is determined to be greater than the initial value. This behaviour is contrary to that found with the material exposed to carbonation [25].

**Table 4.** Results of the galvanostatic pulse used for the concrete from fly ash concrete with and without exposure to CO<sub>2</sub>.

	R <sub>Ω</sub> (Ω)	R <sub>p</sub> (kΩ*cm <sup>2</sup> )
Fly ash concrete carbonated		
0 hours	321	26.65
1000 hours	254	13.45
2000 hours	128	6.21
Fly ash concrete without exposure to carbonation		
0 hours	854	49.25
1000 hours	921	62.15
2000 hours	968	82.14

The evaluation of concrete using the galvanostatic pulse technique shows that the potential response increases as the level of assessment progresses over time for steel with activated slag exposed to conditions of very low CO<sub>2</sub> (natural environment). This same behaviour is observed in the fly ash concrete (Figure5). Table 5 shows the electrochemical conditions of steel in contact with the concrete alternative. The resistance value of the electrolyte concrete has some variations, which do not have a definite trend. At the beginning of the evaluation, a high increase in this value is observed, but in the intermediate time, this value decreases to values below the concrete evaluated above and then increases slowly. When the measurement time reaches 1500 hours, this increase is again high. However, after the trial, this value decreased compared to the previous measurement. This fluctuation in the measured electrolyte resistance is caused by alkaline reactions in the concrete. For the polarization resistance, there was a significant increase when the evaluation was performed at 500 hours. After this time, the increase was small but with a well-marked tendency, which indicated that with increasing time of assessment, the polarization resistance increased.



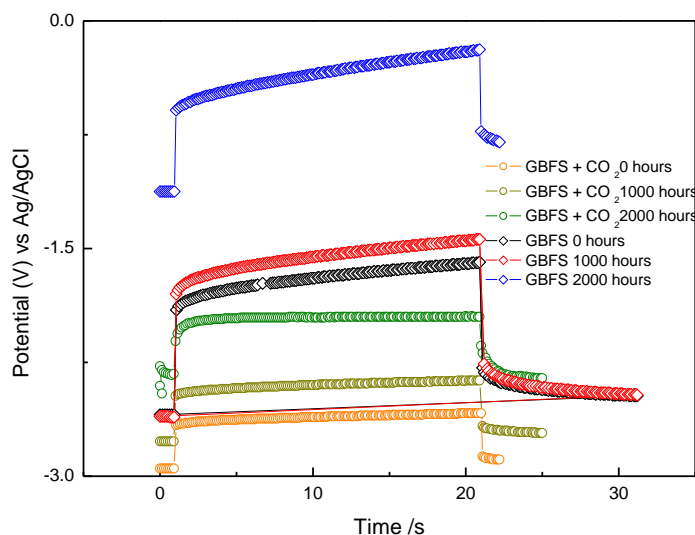


**Figure 5.** Galvanostatic pulse of the concrete GBFS with and without exposure to CO<sub>2</sub>.

When comparing the activated slag concrete submitted to both carbonation and a natural environment, the particular environmental conditions had a higher response value of the electrochemical potential; therefore, this material is always has a stronger electrochemical response when exposed to accelerated carbonation because when subjected to accelerated carbonation, the decreased parameters decrease the response curve [26-27].

**Table 5.** Result of the galvanostatic pulse response used for concrete GBFS with and without CO<sub>2</sub>.

Nivel	R <sub>Ω</sub> (Ω*cm <sup>2</sup> )	R <sub>p</sub> (kΩ*cm <sup>2</sup> )
GBFS carbonated		
0 hours	425	198.4
1000 hours	395	112.6
2000 hours	324	63.2
GBFS without carbonated		
0 hours	492	194.5
1000 hours	372	232.4
2000 hours	448	247.8

With the configuration described above we can see that for our study is only necessary to know the values of ohmic resistance (R<sub>Ω</sub>) and polarization resistance (R<sub>p</sub>), to determine the electrochemical behavior of concrete alternative. Was determined the effect of CO<sub>2</sub> in the analyzed system it produces carbonation in reinforced concrete structures obtained from alternative cementitious materials, so its use is restricted, not to be used in reinforced concrete structures in places with high levels of CO<sub>2</sub> such

as city centers and parking buildings, The effect of the accelerated carbonation process in the fly ash, corresponds to higher porosity to the activating solution/fly ash ratio, also, having determined that a mixture of fly ash cementitious 100% compared with the steel slag carbonation amplification due to the hydrating reaction and subsequent reduction of the alkaline reserve. Finally; it has been found that the rate of carbonation depends on the type of cement, in the case of the steel slag mixtures with higher amount of calcium hydroxide is obtained and therefore greater alkaline reserve.

#### 4. CONCLUSIONS

The electrochemical study of the reinforced concrete subjected to accelerated carbonation and a natural environment measured the open circuit potential and compared the values of the specific GBFS with those obtained in the FA concrete carbonation state. In both cases, the end-of-test steels are in the active state. Under conditions of natural exposure,  $R_p$  increases in both types of concrete, although the steel embedded in the GBFS natural environment had  $R_p$  values up to 3 times higher than the concrete FA. A tendency to stabilize the value of  $R_p$  is also observed in GBFA concrete uncarbonated between 1000 and 2000 hours of operation. Conversely, in the specific FA, there was an increasing trend throughout the process. This result could indicate that the final test age in both cases generated a passive film and is stable.

#### ACKNOWLEDGEMENTS

This research was supported by "Vicerrectoría de investigaciones de la Universidad Militar Nueva Granada" under contract ING 1572.

#### References

1. B. Elsener, H. Wojtas, and H. Bohni, *Proc. Inter. Conf.* 1 (1994) 236
2. S. Sathiyarayanan, P. Natarajan, K. Saravanan, S. Srinivasan, and G. Venkatachari, *Cem. Concr. Compos.* 28(2006) 630
3. V. Karpagam, S. Sathiyarayanan, G. Venkatachari, *Curr. Appl Phys.* 8 (2008) 93
4. K. Kamaraj, S. Sathiyarayanan, G. Venkatachari, *Prog. Org. Coat.* 64 (2009) 67
5. W. Aperador, R. Mejía de Gutiérrez, D.M. Bastidas, *Corros. Sci.* 51 (2009) 2027
6. R. Montoya, W. Aperador, D.M. Bastidas, *Corros. Sci.* 51 (2009) 2857
7. R. Neves, B. Sena da Fonseca, F. Branco, J. de Brito, A. Castela, M.F. Montemor, *Constr. Build. Mater.* 82 (2015) 304
8. B.G. Salvoldi, H. Beushausen, M.G. Alexander, *Constr. Build. Mater.* 85 (2015) 30
9. S.-H. Han, W.-S. Park, E.-I. Yang, *Constr. Build. Mater.* 48 (2013) 1045
10. F. Puertas, C. Varga, M.M. Alonso, *Cem. Concr. Compos.* 53 (2014) 279
11. M. K. Mohammed, A. R. Dawson, N. H. Thom, *Constr. Build. Mater.* 50 (2014)
12. G. S. Ryu, Y. B. Lee, K. T. Koh, Y. S. Chung, *Constr. Build. Mater.* 47 (2013) 409
13. W. K. Part, M. Ramli, C. B. Cheah, *Constr. Build. Mater.* 77 (2015) 370
14. G. Kovalchuk, A. Fernández-Jiménez, A. Palomo, *Fuel.* 86 (2007) 315
15. N. Marjanović, M. Komljenović, Z. Baščarević, V. Nikolić, R. Petrović, *Ceram. Int.* 41 (2015) 1421
16. M. Chi, *Constr. Build. Mater.* 35 (2012) 240

17. M. L. Gualtieri, M. Romagnoli, S. Pollastri, A. F. Gualtieri, *Cem. Concr. Res*, 67 (2015) 259
18. M. Izquierdo, X. Querol, C. Phillipart, D. Antenucci, M. Towler, *J. Hazard. Mater.* 176 (2010) 623
19. S. Chen, M. Wu, S. Zhang, *J. Nucl. Mater.* 402 (2010) 173
20. M.A.M. Ariffin, M.A.R. Bhutta, M.W. Hussin, M. Mohd Tahir, Nor Aziah, *Constr. Build. Mater.* 43 (2013) 80
21. V. Maruthapandian, V. Saraswathy, *Procedia Eng*, 86 (2014) 623
22. M. Chi, R. Huang, *Constr. Build. Mater.* 40 (2013)291
23. A. Natali Murri, W.D.A. Rickard, M.C. Bignozzi, A. van Riessen, *Cement Concrete Res.* 43 (2013)51
24. N Birbilis, K.M Nairn, M Forsyth. *Electrochim Acta*, 49 (2004) 4331
25. M. Holloway, J.M. Sykes, *Corros Sci*, 47 (2005) 3097
26. A. Poursaee, C.M. Hansson, *Corros Sci*, 50 (2008)2739
27. A. Poursaee, *Electrochim Acta*, 55 (2010) 1200

© 2015 The Authors. Published by ESG ([www.electrochemsci.org](http://www.electrochemsci.org)). This article is an open access article distributed under the terms and conditions of the Creative Commons Attribution license (<http://creativecommons.org/licenses/by/4.0/>).